

# Symmetry-breaking transitions in quiescent and moving solitons in fractional couplers

Dmiry V. Strunin<sup>1</sup> and Boris A. Malomed<sup>2,3</sup>

<sup>1</sup>*School of Mathematics, Physics and Computing,  
University of Southern Queensland, Toowoomba, Queensland 4350, Australia*

<sup>2</sup>*Department of Physical Electronics, School of Electrical Engineering,  
Faculty of Engineering, and Center for Light-Matter Interaction,  
Tel Aviv University, P.O.B. 39040, Tel Aviv, Israel*

<sup>3</sup>*Instituto de Alta Investigación, Universidad de Tarapacá, Casilla 7D, Arica, Chile*

We consider phase transitions, in the form of spontaneous symmetry breaking (SSB) bifurcations of solitons, in dual-core couplers with fractional diffraction and cubic self-focusing acting in each core, characterized by Lévy index  $\alpha$ . The system represents linearly-coupled optical waveguides with the fractional paraxial diffraction or group-velocity dispersion (the latter system was used in a recent experiment, which demonstrated the first observation of the wave propagation in an effectively fractional setup). By dint of numerical computations and variational approximation (VA), we identify the SSB in the fractional coupler as the bifurcation of the subcritical type (i.e., the symmetry-breaking phase transition of the first kind), whose subcriticality becomes stronger with the increase of fractionality  $2 - \alpha$ , in comparison with very weak subcriticality in the case of the non-fractional diffraction,  $\alpha = 2$ . In the Cauchy limit of  $\alpha \rightarrow 1$ , it carries over into the *extreme* subcritical bifurcation, manifesting backward-going branches of asymmetric solitons which never turn forward. The analysis of the SSB bifurcation is extended for moving (tilted) solitons, which is a nontrivial problem because the fractional diffraction does not admit Galilean invariance. Collisions between moving solitons are studied too, featuring a two-soliton symmetry-breaking effect and merger of the solitons.

## I. INTRODUCTION

The Schrödinger equation with the kinetic-energy operator represented by a fractional derivative was first derived by Laskin as a generalization of canonical quantum mechanics [1–3]. The scaled form of the one-dimensional fractional Schrödinger equation in the free space, with the *Lévy index* (LI)  $\alpha$  (so named by Mandelbrot [4]) is

$$i \frac{\partial \psi}{\partial t} = \frac{1}{2} \left( -\frac{\partial^2}{\partial x^2} \right)^{\alpha/2} \psi, \quad (1)$$

where the fractional operator is defined as the *Riesz derivative* [5, 6],

$$\left( -\frac{\partial^2}{\partial x^2} \right)^{\alpha/2} \psi(x) = \frac{1}{2\pi} \int_{-\infty}^{+\infty} dp |p|^\alpha \int_{-\infty}^{+\infty} dx' e^{ip(x-x')} \psi(x'). \quad (2)$$

It is built as a nonlocal operator, produced by the juxtaposition of the direct and inverse Fourier transforms, with the fractional differentiation represented by factor  $|p|^\alpha$  in the Fourier space. In the Laskin's fractional quantum mechanics,  $\alpha$  takes values

$$1 < \alpha \leq 2. \quad (3)$$

The limit of  $\alpha = 2$  corresponds to the canonical Schrödinger equation, with operator (2) reducing to the normal second derivative. The case of  $\alpha = 1$  (the “square root of the Laplacian”) is known as the Cauchy driver [7, 8], which occurs, in particular, in the fractional equation for a photonic wave function [9]. Further, it was found that the original LI range (3) may be expanded to  $0 < \alpha \leq 2$  [9].

It is relevant to mention that there are other definitions of the fractional-order differentiation, such as the Caputo derivative [2], but the derivation of the fractional Schrödinger equation by Laskin yields the model with the Riesz derivative [1, 3]. The nonlocal character of the fractional-derivative operators produces essentially nontrivial consequences in bounded domains, with the respective boundary conditions [8, 10]. In particular, different definitions of the fractional derivative produce essentially non-equivalent results in the case of boundary conditions and under the action of external potentials.

While experimental realization of the fractional quantum mechanics is still missing, it was proposed to emulate it by means of the classical wave propagation in photonics, utilizing the commonly known similarity of the Schrödinger equation and the equation for the paraxial propagation of optical beams [11, 12]. The theoretically elaborated setup

for the emulation of the fractional diffraction is based on the  $4f$  optical configuration, which performs the spatial Fourier decomposition of the beam by means of a lens, then carries the beam through an appropriately shaped phase plate to impart the local phase shift which emulates the action of the fractional diffraction as per Eq. (2), and finally retrieves the beam from its Fourier decomposition, using another lens [11]. Other emulations of the fractional quantum mechanics were proposed in Lévy crystals [13] and polariton condensates [14].

Very recently, the first *experimental realization* of the effective fractional group-velocity dispersion (rather than transverse diffraction) in a fiber-laser setup has been reported [15]. While the fractional dispersion acts in the temporal domain, its experimental emulation was carried out by means of a  $4f$  setup similar to the one outlined above, with the difference that the lenses performed the spectral decomposition of the optical signal and inverse recombination. To avoid misunderstanding, it is relevant to stress that the temporal variable plays the role of an efficient coordinate in optical fibers, while the evolution variable is the propagation distance. Therefore, the effective fractional dispersion reported in Ref. [15] emulates the temporal counterpart of the fractional diffraction (cf. Ref. [16]), but not a fractional derivative with respect to the evolution variable, which occurs in various models of anomalous diffusion [17, 18]. Of course, a caveat is that the proposed and reported realizations of the fractional diffraction and dispersion in optics actually report the simulation of these effects by light, but not their direct action.

Theoretical studies of models with the fractional diffraction were developed by including external potentials [in particular, parity-time ( $\mathcal{PT}$ ) symmetric ones [19]-[24]] and studying the propagation of Airy waves in the two-dimensional geometry, with the fractional-diffraction operator  $(-\partial^2/\partial x^2 - \partial^2/\partial y^2)^{\alpha/2}$  [25, 26]. The implementation of the fractional diffraction/dispersion in optical waveguides makes it natural to include the self-focusing Kerr nonlinearity of the material, which leads to the consideration of fractional nonlinear Schrödinger equations (FNLSEs) [27].

The work based on FNLSEs has produced many theoretical results, including the modulational instability of continuous waves [28], critical or supercritical collapse [29], and diverse species of solitons [30]-[27]. These are quasi-linear “accessible solitons” [33, 34], gap solitons maintained by lattice potentials [38]-[42], solitary vortices [43-45], multi-peak modes [46]-[49], clusters [50], discrete solitons [51], and dark modes [52]. Solitons produced by the interplay of the fractional diffraction and quadratic nonlinearity were predicted too [53, 54], as well as dissipative solitons produced by the fractional complex Ginzburg-Landau equation [55].

A generic effect produced by self-trapping nonlinearity is spontaneous symmetry breaking (SSB) in double-well potentials [57]. SSB phenomenology in such settings was studied in detail theoretically [58]-[63] and experimentally [64]-[67] in diverse physical settings. Recently, the theoretical analysis was extended for nonlinear systems combining the fractional diffraction and symmetric potentials [68]-[71]. An appropriate platform for the realization of SSB in the form of two-component solitons with broken symmetry between the components is offered by dual waveguides, which are often represented by double-core optical fibers [72, 73]. The transition from symmetric to asymmetric two-component solitons, i.e., the *SSB bifurcation* in such fibers, was studied in detail theoretically [74]-[79], and it was recently demonstrated in an experiment [80]. In another recent work [81], some families of symmetric and asymmetric solitons were found in the double-core system with fractional diffraction.

The objective of the present work is to identify the SSB bifurcation of two-component solitons in the fractional dual-core waveguide, i.e., the corresponding symmetry-breaking phase transition. We do this analytically, by means of the variational approximation (VA), and in a systematic numerical form. An essential finding is that *deeper* system’s fractionality [i.e., smaller LI  $\alpha$  in Eq. (2)] enhances the *subcritical* character [82] of the bifurcation. In other words, the fractionality makes the SSB of the two-component solitons a more strongly pronounced phase transition of the first kind.

An essential peculiarity of the fractional diffraction is that it does not admit the Galilean invariance. Therefore, the generation of moving solitons and the consideration of the SSB bifurcation for them is a nontrivial problem, which we address here too, and which was not considered previously. Collisions between moving solitons are studied too

Thus, we address the system of linearly-coupled FNLSEs with the cubic self-focusing nonlinearity,

$$\begin{aligned} i \frac{\partial u_1}{\partial t} &= \frac{1}{2} \left( -\frac{\partial^2}{\partial x^2} \right)^{\alpha/2} u_1 - |u_1|^2 u_1 - u_2, \\ i \frac{\partial u_2}{\partial t} &= \frac{1}{2} \left( -\frac{\partial^2}{\partial x^2} \right)^{\alpha/2} u_2 - |u_2|^2 u_2 - u_1, \end{aligned} \quad (4)$$

where the coupling coefficient in front of terms  $-u_2$  and  $-u_1$  is fixed to be 1 by means of scaling. The only irreducible control parameter of the system is LI  $\alpha$ . In terms of optics, Eqs. (4) describe a pair of parallel planar waveguides coupled by tunneling of light. In this case,  $t$  and  $x$  are, respectively, the propagation distance and transverse coordinate. The same system realized in the temporal domain, i.e., with  $x$  standing for the reduced time [83], may be construed as a model of a laser built of dual-core fibers with the effective fractional dispersion, following the experimental method reported in Ref. [15]. The possibility of using dual-core fibers in lasers is a well-known option [84].

There may also be a possibility to consider Eqs. (4) as a system of coupled Gross-Pitaevskii equations for a Bose-Einstein condensate of quantum particles governed by the fractional Schrödinger equations and filling a pair of parallel cigar-shaped traps, which are linearly coupled by tunneling of the particles. In that case,  $t$  is time and  $x$  is the coordinate along the traps. However, the derivation of such a mean-field model for the condensate requires accurate analysis, which should be a subject of a separate work. In particular, it is necessary to check if collisional effects in this system may be properly represented by the usual mean-field cubic terms. Experimental realization of the system may be a challenging objective too.

The presentation is organized below as follows. The framework for the construction of soliton solutions and analysis of their stability and dynamics are presented in Section 2. The analytical approach, based on the VA, is developed in Section 3. Numerical results for quiescent and moving solitons are summarized in Section 4. The work is concluded by Section 5.

## II. THE FRAMEWORK FOR SOLITON SOLUTIONS

Stationary-state solutions to Eq. (4) with propagation constant  $k$  (in the application to BEC,  $-k$  is the chemical potential) are looked for as

$$u_{1,2}(x, t) = U_{1,2}(x)e^{ikt}, \quad (5)$$

with real functions  $U_{1,2}(x)$  satisfying equations

$$\begin{aligned} kU_1 + \frac{1}{2} \left( -\frac{\partial^2}{\partial x^2} \right)^{\alpha/2} U_1 - U_1^3 - U_2 &= 0, \\ kU_2 + \frac{1}{2} \left( -\frac{\partial^2}{\partial x^2} \right)^{\alpha/2} U_2 - U_2^3 - U_1 &= 0. \end{aligned} \quad (6)$$

Taking into regard that  $U_{1,2}(x)$  are even functions of  $x$  and using the definition of the fractional derivative given by Eq. (2), the explicit form of Eq. (6) can be written as

$$\begin{aligned} kU_1 + \frac{1}{2\pi} \int_0^{+\infty} p^\alpha dp \int_{-\infty}^{+\infty} \cos(px) \cos(px') U_1(x') dx' - U_1^3 - U_2 &= 0, \\ kU_2 + \frac{1}{2\pi} \int_0^{+\infty} p^\alpha dp \int_{-\infty}^{+\infty} \cos(px) \cos(px') U_2(x') dx' - U_2^3 - U_1 &= 0. \end{aligned} \quad (7)$$

We consider values of  $\alpha$  in the interval of

$$1 < \alpha \leq 2, \quad (8)$$

as it is well known that, at  $\alpha \leq 1$ , the FNLSE gives rise to the collapse (critical collapse at  $\alpha = 1$ , and supercritical at  $\alpha < 1$ ) [27, 29].

In the case of the normal diffraction,  $\alpha = 2$ , obvious solutions of Eq. (6) in the form of symmetric solitons is

$$U_1 = U_2 = \sqrt{2(k-1)} \operatorname{sech} \left( \sqrt{2(k-1)} x \right). \quad (9)$$

The norm (power) of this solution is

$$N = \int_{-\infty}^{+\infty} \left[ (U_1(x))^2 + (U_2(x))^2 \right] dx = 4\sqrt{2(k-1)}. \quad (10)$$

With the increase of  $N$ , the symmetric states become unstable through SSB, and stable asymmetric solitons appear. While there are no exact solutions for the asymmetric solitons, the SSB point, at which they emerge, can be found exactly for  $\alpha = 2$  [74]:

$$(N_{\text{SSB}})_{\text{exact}} (\alpha = 2) = 8/\sqrt{3}. \quad (11)$$

On the other hand, the VA predicts this point at

$$(N_{\text{SSB}})_{\text{VA}} (\alpha = 2) = 2\sqrt{6} \approx 4.899 \quad (12)$$

[72, 79], the relative error of this result being  $\simeq 6\%$ .

Asymmetry of the solitons produced by the SSB bifurcation is defined by parameter

$$\Theta = N^{-1} \int_{-\infty}^{+\infty} [(\mathbf{u}_1(x))^2 - (\mathbf{u}_2(x))^2] dx. \quad (13)$$

The bifurcation is characterized by diagrams which displays  $\Theta$  as functions of  $k$  or  $N$  [see, in particular, Fig. 3 below].

Solutions of Eq. (4) for moving solitons, i.e., obliquely propagating light beams with slope  $c$  in the planar waveguide, are sought for as

$$\mathbf{u}_{1,2} = \mathbf{u}_{1,2}(\xi \equiv x - ct, t). \quad (14)$$

Accordingly, Eq. (4) is rewritten in terms of  $(\xi, t)$  as

$$\begin{aligned} i \frac{\partial \mathbf{u}_1}{\partial t} - ic \frac{\partial \mathbf{u}_1}{\partial \xi} &= \frac{1}{2} \left( -\frac{\partial^2}{\partial \xi^2} \right)^{\alpha/2} \mathbf{u}_1 - |\mathbf{u}_1|^2 \mathbf{u}_1 - \mathbf{u}_2, \\ i \frac{\partial \mathbf{u}_2}{\partial t} - ic \frac{\partial \mathbf{u}_2}{\partial \xi} &= \frac{1}{2} \left( -\frac{\partial^2}{\partial \xi^2} \right)^{\alpha/2} \mathbf{u}_2 - |\mathbf{u}_2|^2 \mathbf{u}_2 - \mathbf{u}_1. \end{aligned} \quad (15)$$

Solutions to Eq. (15) are further looked for as  $\mathbf{u}_{1,2}(\xi, t) = \mathbf{U}_{1,2}(\xi) e^{ikt}$  [cf. Eq. (5)], with complex functions  $\mathbf{U}_{1,2}(\xi)$  satisfying the following system of stationary equations:

$$\begin{aligned} k\mathbf{U}_1 + ic \frac{d\mathbf{U}_1}{d\xi} + \frac{1}{2} \left( -\frac{d^2}{d\xi^2} \right)^{\alpha/2} \mathbf{U}_1 - |\mathbf{U}_1|^2 \mathbf{U}_1 - \mathbf{U}_2 &= 0, \\ k\mathbf{U}_2 + ic \frac{d\mathbf{U}_2}{d\xi} + \frac{1}{2} \left( -\frac{d^2}{d\xi^2} \right)^{\alpha/2} \mathbf{U}_2 - |\mathbf{U}_2|^2 \mathbf{U}_2 - \mathbf{U}_1 &= 0. \end{aligned} \quad (16)$$

The stability of solitons was addressed by considering solutions including small perturbations  $\mathbf{a}_{1,2}$  and  $\mathbf{b}_{1,2}$ ,

$$\mathbf{u}_{1,2}(x, t) = [\mathbf{U}_{1,2}(x) + \mathbf{a}_{1,2}(x) e^{\lambda t} + \mathbf{b}_{1,2}^*(x) e^{\lambda^* t}] e^{ikt}, \quad (17)$$

where  $\lambda$  is the instability growth rate, and  $*$  stands for the complex conjugate. The linearization of Eq. (4) for the perturbations leads the system of the corresponding Bogoliubov – de Gennes equations:

$$\begin{aligned} \left[ -(k - i\lambda) - \frac{1}{2} \left( -\frac{d^2}{d\xi^2} \right)^{\alpha/2} + 2|\mathbf{U}_{1,2}|^2 \right] \mathbf{a}_{1,2} + \mathbf{U}_{1,2}^2 \mathbf{b}_{1,2} + \mathbf{a}_{2,1} &= 0, \\ \left[ -(k + i\lambda) - \frac{1}{2} \left( -\frac{d^2}{d\xi^2} \right)^{\alpha/2} + 2|\mathbf{U}_{1,2}|^2 \right] \mathbf{b}_{1,2} + (\mathbf{U}_{1,2}^*)^2 \mathbf{a}_{1,2} + \mathbf{b}_{2,1} &= 0. \end{aligned} \quad (18)$$

The stability condition is that solutions of Eq. (18) must produce only eigenvalues with  $\text{Re}(\lambda) = 0$  [85, 89]. Below, the prediction for the stability of the solitons, provided by these equations, is corroborated by direct simulations of the evolution of perturbed solitons.

### III. THE VARIATIONAL APPROXIMATION (VA)

To apply VA, we note that Eq. (7) can be derived from the Lagrangian,

$$L = \int_{-\infty}^{+\infty} \left[ \frac{k}{2} (\mathbf{u}_1^2 + \mathbf{u}_2^2) \right] dx + H, \quad (19)$$

with Hamiltonian

$$\begin{aligned} H &= \int_{-\infty}^{+\infty} \left\{ -\frac{1}{4} [\mathbf{u}_1^4(x) + \mathbf{u}_2^4(x)] - \mathbf{u}_1(x) \mathbf{u}_2(x) \right\} dx \\ &+ \frac{1}{4\pi} \int_0^{+\infty} p^\alpha dp \int_{-\infty}^{+\infty} dx \int_{-\infty}^{+\infty} dx' \cos(p(x - x')) [\mathbf{u}_1(x) \mathbf{u}_1(x') + \mathbf{u}_2(x) \mathbf{u}_2(x')], \end{aligned} \quad (20)$$

cf. Ref. [45]. The ansatz for the asymmetric soliton can be adopted in the simple form, which follows the pattern of the above-mentioned solution (9):

$$u_1(x) = \sqrt{\frac{N}{2W}} (\cos \chi) \operatorname{sech} \left( \frac{x}{W} \right), u_2(x) = \sqrt{\frac{N}{2W}} (\sin \chi) \operatorname{sech} \left( \frac{x}{W} \right), \quad (21)$$

where variational parameters are width  $W$  and norm-distribution angle  $\chi$ , while  $N$  is considered as a given total norm. The asymmetry parameter (13) corresponding to the ansatz is

$$\Theta_{VA} = \cos(2\chi) \equiv \sqrt{1 - S^2}, \quad (22)$$

$$S \equiv \sin(2\chi) \quad (23)$$

(parameter  $S$  is used below). The substitution of ansatz (21) in Lagrangian defined by Eqs. (19) and (20) yields

$$\begin{aligned} L_{VA} = & \frac{N}{2}k - \frac{N^2}{12W} \left( 1 - \frac{1}{2} \sin^2(2\chi) \right) - \frac{N}{2} \sin(2\chi) \\ & + (1 - 2^{1-\alpha}) \Gamma(1 + \alpha) \zeta(\alpha) \frac{N}{2(\pi W)^\alpha}, \end{aligned} \quad (24)$$

where  $\Gamma$  and  $\zeta$  are the Gamma- and zeta-functions. Parameters of the asymmetric solitons are predicted by the Euler-Lagrange equations,

$$\frac{\partial L_{VA}}{\partial W} = \frac{\partial L_{VA}}{\partial (\sin(2\chi))} = 0, \quad (25)$$

which amount to relation  $W = (N/6) \sin(2\chi)$ , and an equation for  $S \equiv \sin(2\chi)$ :

$$S^{\alpha-1} \left( 1 - \frac{S^2}{2} \right) = \frac{\alpha}{\pi^\alpha} (1 - 2^{1-\alpha}) \Gamma(1 + \alpha) \zeta(\alpha) \left( \frac{6}{N} \right)^\alpha. \quad (26)$$

In particular, the threshold at which SSB takes place, giving rise to families of asymmetric solutions which branch off from symmetric ones, that correspond to  $S = 1$ , is produced by the substitution of  $S = 1$  in Eq. (26):

$$(N_{SSB})_{VA}(\alpha) = \frac{6}{\pi} [2\alpha (1 - 2^{1-\alpha}) \Gamma(1 + \alpha) \zeta(\alpha)]^{1/\alpha}. \quad (27)$$

In the case of  $\alpha = 2$ , expression (27) exactly reduces to Eq. (12). In the opposite limit of  $\alpha - 1 \rightarrow +0$  [see Eq. (8)], Eq. (27) yields

$$(N_{SSB})_{VA}(\alpha \rightarrow 1) = 12\pi^{-1} \ln 2 \approx 2.648. \quad (28)$$

Finally, the VA prediction for the asymmetry dependence on the norm,  $\Theta(N)$ , is obtained, in an implicit form, as a combination of Eqs. (22), (23), and (26):

$$(1 - \Theta_{VA}^2)^{(\alpha-1)/2} (1 + \Theta_{VA}^2) = \frac{2\alpha}{\pi^\alpha} (1 - 2^{1-\alpha}) \Gamma(1 + \alpha) \zeta(\alpha) \left( \frac{6}{N} \right)^\alpha. \quad (29)$$

This relation takes an explicit form in the limit of  $\alpha \rightarrow 1$ :

$$\Theta_{VA}(N; \alpha \rightarrow 1) = \sqrt{\frac{(N_{SSB})_{VA}(\alpha \rightarrow 1)}{N} - 1}, \quad (30)$$

where  $(N_{SSB})_{VA}(\alpha \rightarrow 1)$  is the value given by Eq. (28). Dependence (30) is displayed below in Fig. 3, and the predictions produced by Eqs. (29) and (27) are compared with numerical results in Fig. 3.

## IV. NUMERICAL RESULTS

### A. The spontaneous-symmetry-breaking (SSB) bifurcation of stationary states and their stability

Soliton solutions of Eq. (7) were produced by means of the squared-operator iteration method [85, 86]. Then, the spectrum of stability eigenvalues  $\lambda$  was produced solving Eq. (18) by means of the Fourier collocation method. Both

algorithms were realized in the Matlab shell, as outlined in Ref. [85]. Direct simulations of Eq. (4) were performed by means of the pseudospectral method [85, 90–92],

A typical profile of an asymmetric soliton is presented in Fig. 1(a). Panels (b) and (c) of the figure demonstrate that this soliton is unstable, spontaneously transforming into a robust breather, which is a dynamical state effectively symmetrized by persistent oscillations between its two components. The shape of stable asymmetric soliton is similar to that in Fig. 1. As for symmetric solitons, those ones which are unstable spontaneously turn into stable asymmetric ones, with residual internal oscillations (not shown here in detail).

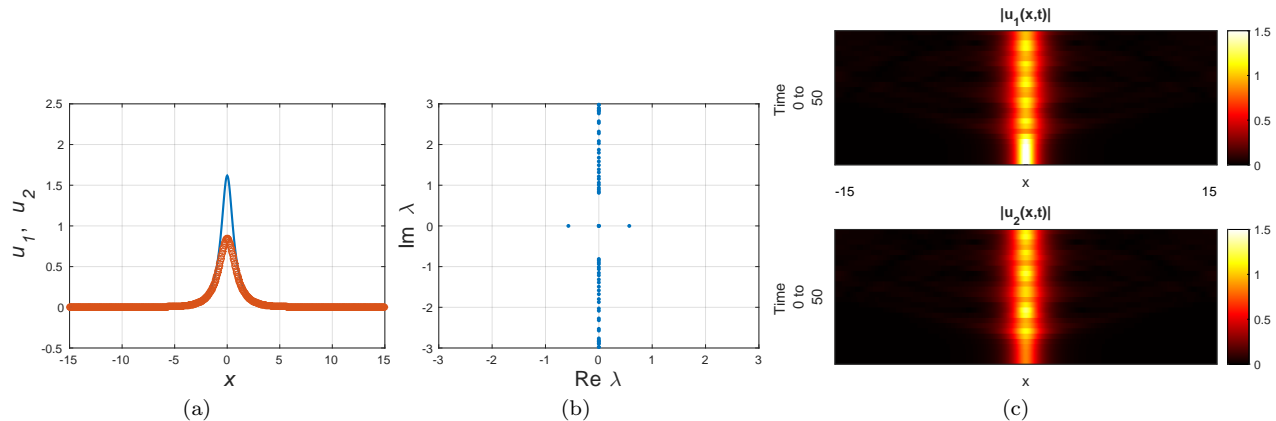


FIG. 1. The stationary profile of an unstable asymmetric soliton (a), its spectrum of perturbation eigenvalues (b), and perturbed evolution (c), for  $\alpha = 1.6$ ,  $k = 1.8$ , and  $N = 3.729$ . Shapes of stable asymmetric solitons are similar to the one displayed here.

Families of numerically found stationary symmetric and asymmetric solitons, and the SSB bifurcation which couples them, are displayed in Figs. 2 and 3 by respective dependences  $N(k)$  and  $\Theta(N)$ , in the interval of LI values  $1.1 \leq \alpha \leq 2.0$ , cf. Eq. (8) (the numerical solution is technically challenging for  $\alpha < 1.1$  because of slow convergence). The latter figure includes the comparison with the VA prediction, given above by Eq. (29). It is seen that the VA is reasonably accurate, with the relative discrepancy in terms of  $N$  for fixed  $\Theta$  being  $\leq 6\%$  in Fig. 3(a). In particular, the VA results are quite reliable for stable branches  $\Theta(N)$ . In the case of  $\alpha = 2$ , the findings are tantamount to the well-known results for the usual coupler [72, 73].

Note that the (in)stability of all solution branches, as shown in Figs. 2 and 3, complies with the Vakhitov-Kolokolov criterion,  $dN/dk > 0$ , which is the necessary stability condition for self-trapped modes [85, 87]. In particular, the asymmetric solitons belonging to the backward- and forward-going segments of the respective solution branches are stable or not in agreement with the criterion.

Figures 2 and 3(a) demonstrate that, as it might be expected, the increase of the norm leads to destabilization of symmetric solitons and emergence of asymmetric ones via the SSB bifurcation. Similar to the known feature of SSB in the usual coupler ( $\alpha = 2$ ), Fig. 3 shows that the bifurcation is of the subcritical type [82], thus representing a phase transition of the first kind, which admits hysteresis and bistability. The subcritical bifurcation gives rise to branches of asymmetric solitons that originally go in the backward direction (which corresponds to the decrease of  $N$ ), and then turn forward at critical points. These points represent the minimum value of  $N$  at which the asymmetric solitons exist. An essential conclusion suggested by Fig. 3 is that *deeper fractionality*, i.e., larger  $2 - \alpha$ , makes the subcritical character of the SSB bifurcation stronger, while this feature is very weak in the usual case,  $\alpha = 2$ . As an extension of this trend, Fig. 3 shows that, at  $\alpha = 1.2$ , the branch of the asymmetric solitons admits almost no extension past the critical turning point. Additional numerical results demonstrate that, in the explored range of values of  $k$ , the  $\Theta(N)$  curve does not reach the turning point for  $\alpha = 1.1$ . A conjecture is that the SSB bifurcation becomes an *extreme subcritical one*, with no turning points, in the limit of  $\alpha \rightarrow 1$ . Indeed, this feature is explicitly demonstrated by the VA curve produced by Eq. (30), which is plotted in Fig. 3(a).

Note that the first example of the extreme subcritical SSB bifurcation was reported in the model based on the single NLS equation with the usual diffraction and nonlinear double-well potential [88],

$$i \frac{\partial \mathbf{u}}{\partial t} = -\frac{1}{2} \frac{\partial^2 \mathbf{u}}{\partial x^2} - [\delta(x-1) + \delta(x+1)] |\mathbf{u}|^2 \mathbf{u}, \quad (31)$$

where  $\delta$  is the delta-function, with separation 2 between the potential wells fixed by scaling. An exact analytical solution of Eq. (31) produces the extreme subcritical bifurcation, with branches of asymmetric solitons going backward from the bifurcation point,  $N(\Theta = 0) = \frac{2}{3} + \frac{8}{27} \left( \frac{3}{4} + \ln 2 \right) \approx 1.09$ , up to  $N(\Theta = 1) = 1$ , and never turning forward.

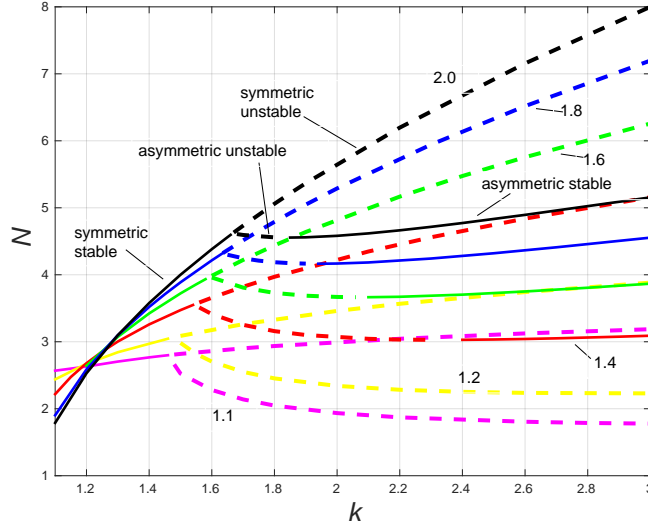


FIG. 2. Norm  $N$  of symmetric and asymmetric solitons plotted versus the propagation constant,  $k$ , at different values of LI  $\alpha$ , as indicated by labels. Solid and dashed lines mark stable and unstable branches, respectively, according to the eigenvalue spectrum produced by Eq. (18).

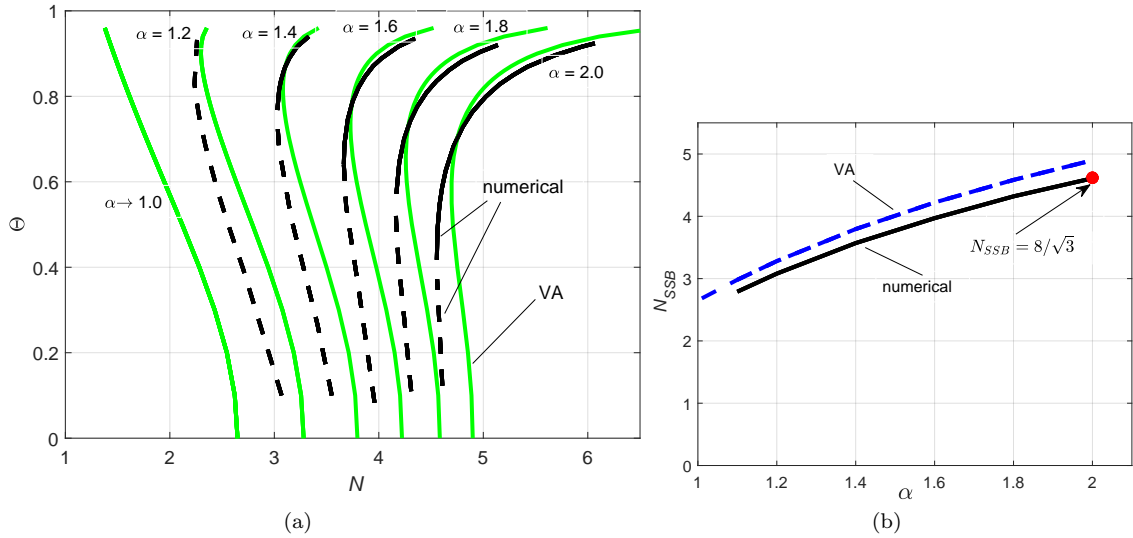


FIG. 3. (a) Symmetry parameter  $\Theta$ , defined as per Eq. (13), versus the norm, for families of asymmetric solitons, at indicated values of LI  $\alpha$ . Plotted are both the numerical results and their analytical counterparts, predicted by VA as per Eq. (29). For  $\alpha \rightarrow 1$ , the VA curve is plotted according to Eq. (30). Solid and dashed segments of the numerically generated branches mark stable and unstable solutions, respectively. (b) The value of the norm at the SSB bifurcation point versus LI  $\alpha$ , as produced by the numerical solution and predicted by VA, see Eq. (27). At  $\alpha = 2$ , the red point shows the exact value (11), which is identical to the corresponding numerically found one. At  $\alpha = 1$ , the VA value is given by Eq. (28).

The basic characteristic of the SSB is the value of the norm,  $N_{SSB}$ , at the bifurcation point, which is predicted by VA as per Eq. (27). The numerically found value is displayed, as a function of  $\alpha$ , along with its VA-predicted counterpart, in Fig. 3(b). The mismatch between the numerical and variational values does not exceed 6%.

In addition to the symmetric and asymmetric solitons, solutions for antisymmetric ones, with  $U_1(x) = -U_2(x)$ , were constructed too, but they are completely unstable (similar to the known situation in the usual coupler, with  $\alpha = 2$  [72, 73]). This conclusion is explained by the fact that the linear-coupling term in Hamiltonian (20), with density  $-U_1(x)U_2(x)$ , is negative for symmetric and asymmetric modes, but positive for the antisymmetric ones, the higher energy (Hamiltonian) implying the instability.

## B. Spontaneous symmetry breaking (SSB) of moving (tilted) solitons

As mentioned above, the incompatibility of the Galilean invariance with the fractional diffraction makes velocity (tilt)  $c$  of the solitons a nontrivial parameter in Eq. (16). First, we address effects of  $c$  on the SSB bifurcation, which was not addressed in previous works. For selected values of  $c$ , bifurcation diagrams produced by the numerical solution of Eq. (16) are displayed in Fig. 4(a), which demonstrates that the bifurcation keeps its subcritical character. The shift of the  $N(k)$  curves to larger  $k$  is similar to the effect of the Galilean boost in the case of the usual diffraction ( $\alpha = 2$ ): in that case, the removal of the velocity terms by means of the boost produces a shift of the propagation constant  $\Delta k = c^2/2$ . For values  $c = 0.4$  and  $0.8$ , which are presented in Fig. 4(a), this expression yields  $\Delta k(c = 0.4) = 0.08$  and  $\Delta k(c = 0.8) = 0.32$ , being close to the shifts observed in Fig. 4(a). A new effect, which is absent in the case of the usual diffraction, is the decrease of norm  $N_{\text{SSB}}$  at the bifurcation point with the increase of  $c$ . It can be explained by the fact that, for complex profile functions  $U_{1,2}(x)$ , in the case of  $c \neq 0$ , the coupling Hamiltonian is  $H_{\text{coupling}} = \int_{-\infty}^{+\infty} \text{Re}\{U_1(x)U_2^*(x)\} dx$ , cf. Eq. (20). Its value is reduced due to averaging of oscillations of the complex integrand. In turn, the relative attenuation of the coupling naturally leads to a decrease of value  $N_{\text{SSB}}$  at the point where the nonlinearity becomes strong enough to initiate the SSB.

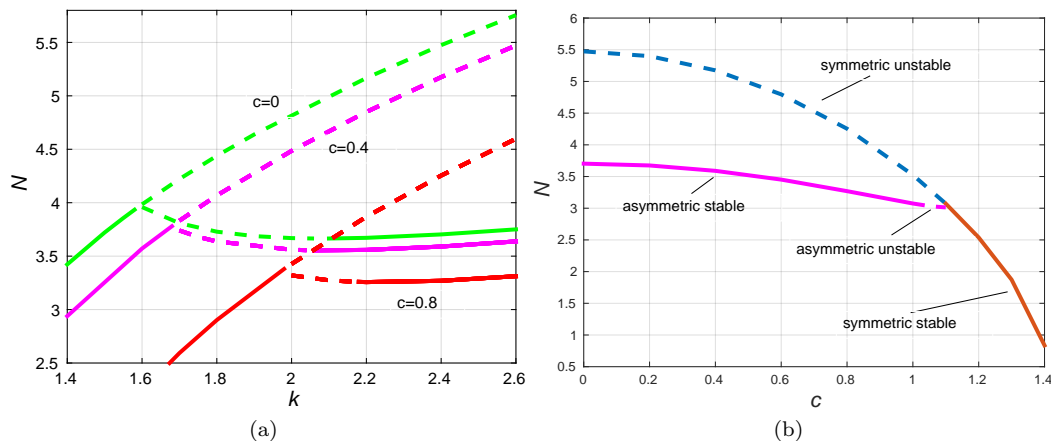


FIG. 4. (a) SSB bifurcation diagrams at LI  $\alpha = 1.6$  for different values of the soliton's speed (tilt)  $c$ . (b) Power  $N$  versus  $c$  for fixed  $\alpha = 1.6$ ,  $k = 2.4$ .

Another manifestation of the effect of  $c$  on the families of stable and unstable symmetric and asymmetric solitons is displayed in Fig. 4(b) for fixed values of LI  $\alpha$  and propagation constant  $k$ . It is seen that tilt  $c$  can be used to switch the optical beams between the asymmetric and symmetric shapes, which may find applications in the design of photonic devices. The trend towards the decrease of  $N$  for large values of  $c$ , especially for the symmetric solitons (for which the two-component structure is not essential, while the fractionality remains a dominant factor), can be explained by noting that rapid oscillations of the complex wave function  $\psi(x)$  caused by large  $c$  make the value of the fractional derivative in Eq. (2) smaller. Therefore, the strength of the self-focusing term (determined by the value of the norm), which is necessary to balance the fractional diffraction in solitons, becomes lower.

## C. Collisions between moving solitons

Once stable solitons are produced in the moving (tilted) state, they can be used to explore collisions of soliton pairs in the coupler [93]. For this purpose, two solitons were numerically constructed as solutions of Eq. (16),  $u_{1,2}^\pm$ , with velocities  $\pm c$ . Then, direct simulations of Eq. (4) were run, with the input in the form of the pair of solitons  $u_{1,2}^\pm(x)$  placed, respectively, at  $x < 0$  and  $x > 0$ , with a sufficiently large distance between them.

Here we focus on the following (most natural) settings for collisions between mutually symmetric solitons, with equal values of the propagation constant,  $k$ : (1) two stable symmetric solitons; (2) two stable asymmetric solitons, with the same  $k$ , in the *flipped* configuration, where soliton  $u_{1,2}^+$  has a larger component  $u_1$  and a smaller one  $u_2$ , and vice versa for  $u_{1,2}^-$  (cf. Ref. [93]); and (3) two stable asymmetric solitons, which are mirror images of each other.

Outcomes of collisions between stable symmetric solitons, at gradually increasing speeds  $\pm c$ , are presented in Fig. 5. In all cases, the colliding solitons bounce back – naturally, remaining far separated for smallest speeds, and approaching



closer to each other for larger  $c$ . Up to the case of  $c = 0.06$ , the entire picture remains fully symmetric, with respect to both the two components in each soliton, and two colliding solitons as well. Next, starting from  $c = 0.08$ , the simulations demonstrate onset of collision-induced SSB, which becomes obvious in the case of  $c = 0.10$ . In this case, the collision breaks the symmetry between the components, as well as between the colliding solitons. In particular, it is worthy to note that the post-collision amplitude of component  $u_2$  in the left soliton is much larger than before the collision. The collision-induced SSB effect is explained by the instability of the transient state formed by the colliding solitons when they are separated by a relatively small distance. A qualitatively similar SSB mechanism was discovered by simulations of soliton-soliton collisions in the single equation with the normal diffraction ( $\alpha = 2$ ) and cubic-quintic nonlinearity [94].

With subsequent growth of  $c$ , the collision picture remains approximately the same as shown in Fig. 5 for  $c = 0.12$  up to  $c = 0.2$  (not shown here in detail). At still larger speeds, the symmetry is gradually recovered, leading, eventually, to practically elastic collisions at  $c \geq 0.34$ , which is a natural outcome of fast collisions [95].

Results of collisions between stable asymmetric solitons in the mutually flipped states, as defined above, are demonstrated in Fig. 6. The general picture is similar to that outlined above for the collisions between symmetric solitons. Namely, at low speeds,  $c \leq 0.04$ , the solitons bounce back, without breaking the symmetry between the colliding ones. In fact, in this case each soliton switches from the intrinsic asymmetric shape into a nearly symmetric one, as concerns the relation between its two components. Then, starting from  $c = 0.06$ , the collision-induced SSB effect sets in, leading to strong symmetry breaking at  $c = 0.1$ , with a dominant  $u_1$  component of the left soliton in the post-collision state. Approximately the same inelastic outcome of the collision persists up to  $c \simeq 0.40$  (not shown here in detail), while the further increase of the speed gradually leads to a transition to quasi-elastic collisions.

The situation when a fully inelastic collision of the mutually flipped asymmetric solitons gives rise to very strong symmetry breaking is additionally illustrated by Fig. 7(a), for the same values of  $\alpha$  and  $k$  as in Fig. 6, and  $c = 0.42$ . It is observed that, in the post-collision state, component  $u_1$  almost vanishes, while nearly all the initial norm is trapped in component  $u_2$  in the form of a quasi-soliton, which performs slow erratic motion. Actually, the dominant component and direction of motion of the emerging mode are selected by the system randomly (as confirmed by additional numerical results), as a result of the above-mentioned instability in the transient state created by the collision.

Lastly, in Fig. 7(b) we present an example of a fully inelastic collision between identical stable asymmetric solitons, i.e., ones in the unflipped configuration. In this case, the solitons merge into a single strongly asymmetric quiescent one, with the same dominant component  $u_1$  as in the original solitons.

## V. CONCLUSION

As a contribution to the quickly developing studies of solitons in systems with fractional diffraction, we have addressed the phenomenology of the SSB (spontaneous symmetry breaking) in the one-dimensional dual-core system, with the Riesz fractional derivative and cubic self-focusing acting in the cores, and linear coupling between the cores. The corresponding system of FNLSEs (fractional nonlinear Schrödinger equations) models tunnel-coupled planar optical waveguides with the fractional diffraction, as well as coupled waveguides with the fractional group-velocity dispersion in the temporal domain (the latter setting was recently realized in the experiment [15], and may be appropriate for the realization of the results predicted in the present work).

By means of systematic numerical computations and the analytical method based on the VA (variational approximation), we have identified the SSB in the system as the bifurcation of the subcritical type, i.e., the phase transition of the first kind. With the increase of the fractionality, i.e., parameter  $2 - \alpha$ , where  $\alpha$  is the LI (Lévy index), the subcritical character of the SSB bifurcations gets stronger pronounced, in comparison with very weak subcriticality in the case of the usual (non-fractional) diffraction,  $\alpha = 2$ . In the limit of  $\alpha \rightarrow 1$ , the bifurcation becomes the *extreme subcritical* one, i.e., with the backward-going branches of asymmetric solitons which never turn forward. The VA produces reasonably accurate results for the SSB, in spite of the complex structure of the system. The (in)stability of families of asymmetric solitons exactly follows the Vakhitov-Kokolov criterion. By means of the numerical method, the study of the SSB bifurcation and families of symmetric and asymmetric solitons has been extended for moving (tilted) ones, which is a nontrivial issue for the fractional system, as it breaks the Galilean invariance. Collisions between moving solitons are systematically studied too, demonstrating another SSB effect, as well as merger of the colliding solitons.

As an extension of the analysis, it may be relevant to consider a similar system of linearly coupled fractional complex Ginzburg-Landau equations, with the objective to predict symmetric and asymmetric dissipative solitons, as well as bound states of such solitons in the respective laser systems, cf. Ref. [96] where a similar analysis was developed in the case of the non-fractional diffraction.

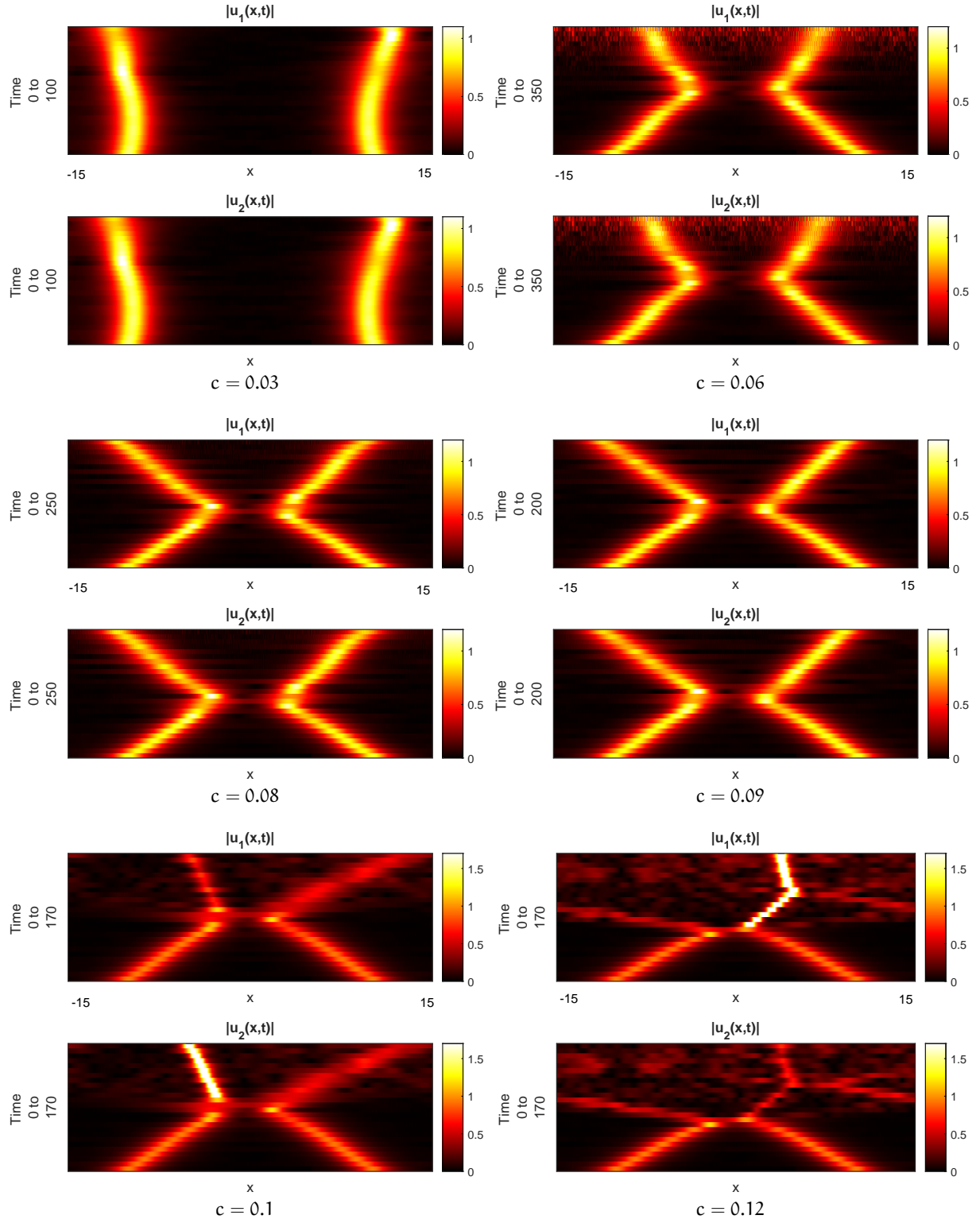


FIG. 5. The onset of SSB in collisions of slowly moving symmetric solitons, with  $\alpha = 1.6$ ,  $k = 1.4$ , and velocities  $\pm c$ . The norms of the solitons are  $N = 3.420$  ( $c = 0.03$ ),  $N = 3.412$  ( $c = 0.06$ ),  $N = 3.404$  ( $c = 0.08$ ),  $N = 3.399$  ( $c = 0.09$ ),  $N = 3.393$  ( $c = \pm 0.10$ ),  $N = 3.380$  ( $c = \pm 0.12$ ).

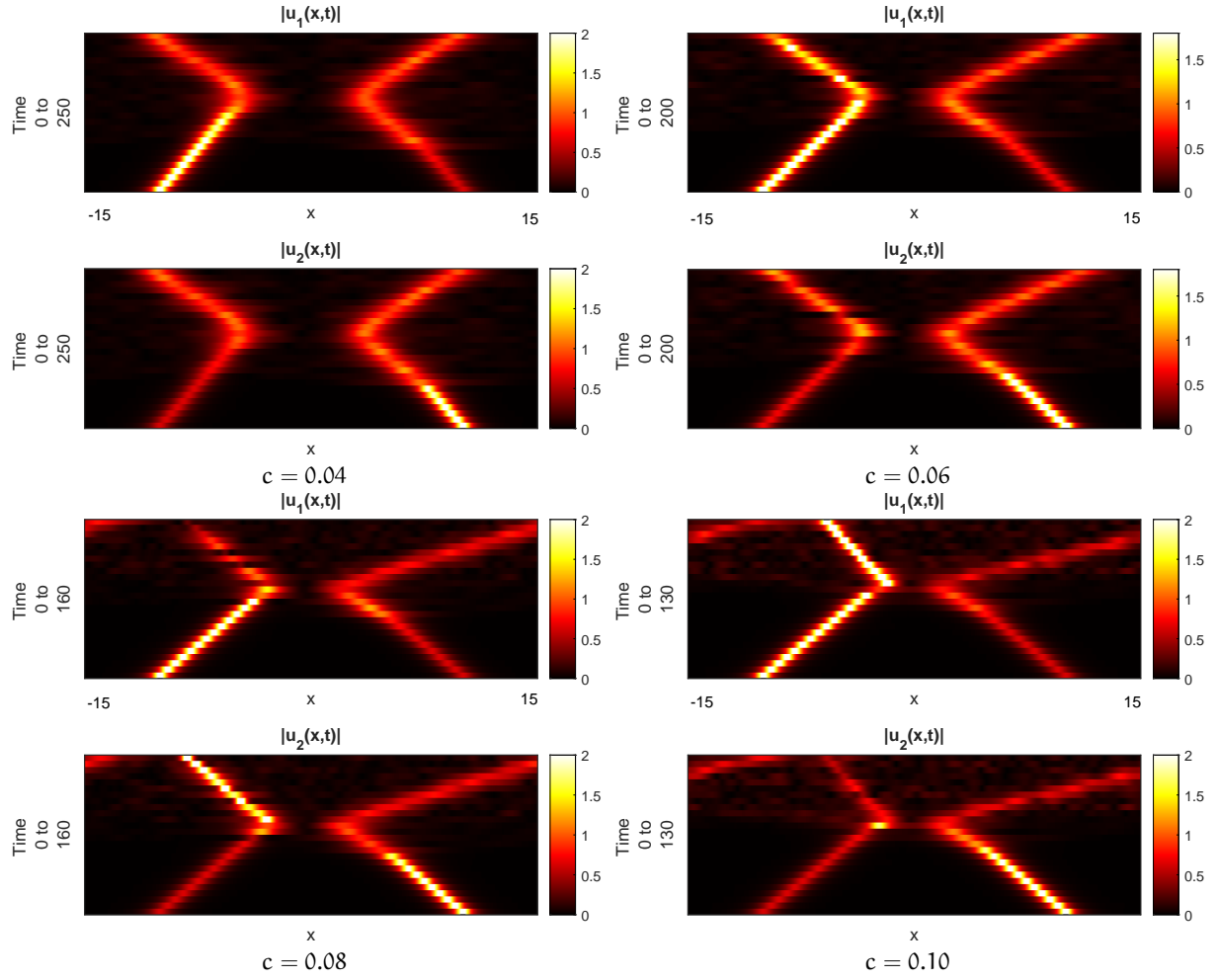


FIG. 6. The gradual onset of SSB in collisions of slowly moving mutually flipped asymmetric solitons, with  $\alpha = 1.6$ ,  $k = 2.6$ , and velocities  $\pm c$ . The norms of the solitons are  $N = 3.749$  ( $c = 0.04$ ),  $N = 3.748$  ( $c = 0.06$ ),  $N = 3.746$  ( $c = 0.08$ ),  $N = 3.744$  ( $c = 0.1$ ), cf. Fig. 5.

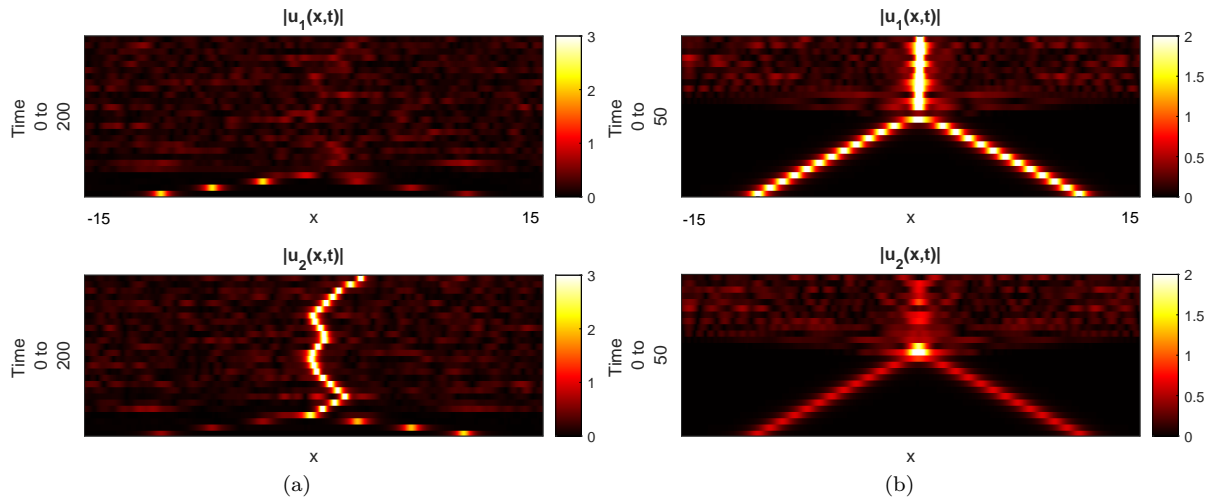


FIG. 7. Examples of strongly inelastic collisions of solitons with  $k = 2.6$  at  $\alpha = 1.6$ . (a) The post-collision dynamics of originally flipped asymmetric solitons for  $c = 0.42$  and  $N = 3.627$ . (b) Merger of asymmetric solitons colliding in the unflipped state, for  $c = 0.4$  and  $N = 3.638$ .

## ACKNOWLEDGMENT

We appreciate a useful discussion with W. B. Cardoso. The work of B.A.M. was supported, in part, by grant No. 1695/22 of the Israel Science Foundation.

- 
- [1] N. Laskin, Fractional quantum mechanics and Lévy path integrals. *Phys. Lett. A* **268**, 298-305 (2000).
- [2] S. I. Muslih, O. P. Agrawal, and D. Baleanu, A fractional Schrödinger equation and its solution, *Int. J. Theor. Phys.* **49**, 1746-1752 (2010).
- [3] N. Laskin, *Fractional quantum mechanics* (World Scientific: Singapore, 2018).
- [4] B. B. Mandelbrot, *The Fractal Geometry of Nature* (W. H. Freeman, New York, 1982).
- [5] O. P. Agrawal, Fractional variational calculus in terms of Riesz fractional derivatives, *J. Phys. A – Math. Theor.* **40**, 6287-6303 (2007).
- [6] M. Cai and C. P. Li, On Riesz derivative, *Fractional Calculus and Applied Analysis* **22**, 287-301 (2019).
- [7] P. Garbaczewski, Cauchy flights in confining potentials, *Physica A* **389**, 936-944 (2010).
- [8] M. Żaba and P. Garbaczewski, Solving fractional Schrödinger-type spectral problems: Cauchy oscillator and Cauchy well, *J. Math. Phys.* **55**, 092103 (2014).
- [9] P. Garbaczewski and V. Stephanovich, Levy flights and nonlocal quantum dynamics, *J. Math. Phys.* **54**, 072103 (2013).
- [10] P. Garbaczewski and V. Stephanovich, Fractional Laplacians in bounded domains: Killed, reflected, censored, and taboo Lévy flights, *Phys. Rev. E* **99**, 042126 (2019).
- [11] S. Longhi, Fractional Schrödinger equation in optics. *Opt. Lett.* **40**, 1117-1120 (2015).
- [12] Y. Zhang, X. Liu, M. R. Belić, W. Zhong, Y. Zhang, M. Xiao, Propagation dynamics of a light beam in a fractional Schrödinger equation, *Phys. Rev. Lett.* **115**, 180403 (2015).
- [13] B. A. Stickler, Potential condensed-matter realization of space-fractional quantum mechanics: The one-dimensional Lévy crystal. *Phys. Rev. E* **88**, 012120 (2013).
- [14] F. Pinsker, W. Bao, Y. Zhang, H. Ohadi, A. Dreismann, and J. J. Baumberg, Fractional quantum mechanics in polariton condensates with velocity-dependent mass. *Phys. Rev. B* **92**, 195310 (2015).
- [15] S. Liu, Y. Zhang, B. A. Malomed, and E. Karimi, Experimental realisations of the fractional Schrödinger equation in the temporal domain, *Nature Comm.* **14**, 222 (2023).
- [16] J. Fujioka, A. Espinosa, and R. F. Rodríguez, Fractional optical solitons, *Phys. Lett. A* **374**, 1126-1134 (2010).
- [17] F. Mainardi, Fractional relaxation-oscillation and fractional diffusion-wave phenomena, *Chaos, Solitons & Fractals* **7**, 1461-1477 (1996).
- [18] Y. M. Lin and C. J. Xu, Finite difference/spectral approximations for the time-fractional diffusion equation, *J. Comput. Phys.* **225**, 1533-1552 (2007).
- [19] Y. Zhang, H. Zhong, M. R. Belić, Y. Zhu, W. Zhong, Y. Zhang, D. N. Christodoulides, M. Xiao,  $\mathcal{PT}$  symmetry in a fractional Schrödinger equation, *Laser Photonics Rev.* **10**(3), 526-531 (2016).
- [20] X. Yao, and X. Liu, Solitons in the fractional Schrödinger equation with parity-time-symmetric lattice potential, *Photonic Res.* **6**, 875-879 (2018).
- [21] P. Li, J. Li, B. Han, H. Ma, and D. Mihalache,  $\mathcal{PT}$ -symmetric optical modes and spontaneous symmetry breaking in the space-fractional Schrödinger equation, *Rom. Rep. Phys.* **71**, 106 (2019).
- [22] Z. Wu, S. Cao, W. Che, F. Yang, X. Zhu, and Y. He, Solitons supported by parity-time-symmetric optical lattices with saturable nonlinearity in fractional Schrödinger equation, *Results Phys.* **19**, 103381 (2020).
- [23] P. Li, B. A. Malomed and D. Mihalache, Symmetry-breaking bifurcations and ghost states in the fractional nonlinear Schrödinger equation with a  $\mathcal{PT}$ -symmetric potential, *Opt. Lett.* **46**, 3267-3270 (2021).
- [24] L. Zeng, J. Shi, X. Lu, Y. Cai, Q. Zhu, H. Chen, H. Long, and J. Li, Stable and oscillating solitons of  $\mathcal{PT}$ -symmetric couplers with gain and loss in fractional dimension, *Nonlinear Dyn.* **103**, 1831-1840 (2021).
- [25] S. He, B. A. Malomed, D. Mihalache, X. Peng, X. Yu, Y. He, and D. Den, Propagation dynamics of abruptly autofocusing circular Airy Gaussian vortex beams in the fractional Schrödinger equation, *Chaos, Solitons & Fractals* **142**, 110470 (2021).
- [26] S. He, B. A. Malomed, D. Mihalache, X. Peng, Y. He, and D. Deng, Propagation dynamics of radially polarized symmetric Airy beams in the fractional Schrödinger equation, *Phys. Lett. A* **404**, 127403 (2021).
- [27] B. A. Malomed, Optical solitons and vortices in fractional media: A mini-review of recent results, *Photonics* **8**, 353 (2021).
- [28] L. Zhang, Z. He, C. Conti, Z. Wang, Y. Hu, D. Lei, Y. Li, and D. Fan, Modulational instability in fractional nonlinear Schrödinger equation, *Commun. Nonlin. Sci. Numer. Simulat.* **48**, 531-540 (2017).
- [29] M. Chen, S. Zeng, D. Lu, W. Hu, and Q. Guo, Optical solitons, self-focusing, and wave collapse in a space-fractional Schrödinger equation with a Kerr-type nonlinearity, *Phys. Rev. E* **98**, 022211 (2018).
- [30] J. Fujioka, A. Espinosa, and R. F. Rodríguez, Fractional optical solitons, *Phys. Lett. A* **374**, 1126-1134 (2010).
- [31] S. Secchi and M. Squassina, Soliton dynamics for fractional Schrödinger equations, *Applicable Analysis*, **93**, 1702-1729 (2014).
- [32] S. Duo and Y. Zhang, Mass-conservative Fourier spectral methods for solving the fractional nonlinear Schrödinger equation, *Computers and Mathematics with Applications* **71**, 2257-2271 (2016).

- [33] W. P. Zhong, M. R. Belić, B. A. Malomed, Y. Zhang, and T. Huang, Spatiotemporal accessible solitons in fractional dimensions, *Phys. Rev. E* **94**, 012216 (2016).
- [34] W. P. Zhong, M. R. Belić, and Y. Zhang, Accessible solitons of fractional dimension, *Ann. Phys.* **368**, 110-116 (2016).
- [35] Y. Hong and Y. Sire, A new class of traveling solitons for cubic fractional nonlinear Schrödinger equations, *Nonlinearity* **30**, 1262-1286 (2017).
- [36] Q. Wang, J. Li, L. Zhang, and W. Xie, Hermite-Gaussian-like soliton in the nonlocal nonlinear fractional Schrödinger equation, *EPL* **122**, 64001 (2018).
- [37] Q. Wang, and Z. Z. Deng, Elliptic Solitons in (1+2)-dimensional anisotropic nonlocal nonlinear fractional Schrödinger equation, *IEEE Photonics J.* **11**, 1-8 (2019).
- [38] C. Huang and L. Dong, Gap solitons in the nonlinear fractional Schrödinger equation with an optical lattice, *Opt. Lett.* **41**, 5636-5639 (2016).
- [39] J. Xiao, Z. Tian, C. Huang, and L. Dong, Surface gap solitons in a nonlinear fractional Schrödinger equation, *Opt. Express* **26**, 2650-2658 (2018).
- [40] L. F. Zhang, X. Zhang, H. Z. Wu, C. X. Li, D. Pierangeli, Y. X. Gao, and D. Y. Fan, Anomalous interaction of Airy beams in the fractional nonlinear Schrödinger equation, *Opt. Exp.* **27**, 27936-27945 (2019).
- [41] L. Dong and Z. Tian, Truncated-Bloch-wave solitons in nonlinear fractional periodic systems, *Ann. Phys.* **404**, 57-64 (2019).
- [42] L. Zeng and J. Zeng, One-dimensional gap solitons in quintic and cubic-quintic fractional nonlinear Schrödinger equations with a periodically modulated linear potential, *Nonlinear Dyn.* **98**, 985-995 (2019).
- [43] P. Li, B. A. Malomed, and D. Mihalache, Vortex solitons in fractional nonlinear Schrödinger equation with the cubic-quintic nonlinearity, *Chaos Solitons Fract.* **137**, 109783 (2020).
- [44] Q. Wang and G. Liang, Vortex and cluster solitons in nonlocal nonlinear fractional Schrödinger equation, *J. Optics* **22**, 055501 (2020).
- [45] H. Sakaguchi and B. A. Malomed, One- and two-dimensional solitons in spin-orbit-coupled Bose-Einstein condensates with fractional kinetic energy, *J. Phys. B: At. Mol. Opt. Phys.* **55**, 155301 (2022).
- [46] L. Zeng and J. Zeng, One-dimensional solitons in fractional Schrödinger equation with a spatially periodical modulated nonlinearity: nonlinear lattice, *Opt. Lett.* **44**, 2661-2664 (2019).
- [47] Y. Qiu, B. A. Malomed, D. Mihalache, X. Zhu, X. Peng, and Y. He, Stabilization of single- and multi-peak solitons in the fractional nonlinear Schrödinger equation with a trapping potential, *Chaos Solitons Fract.* **140**, 110222 (2020).
- [48] P. Li, B. A. Malomed, and D. Mihalache, Metastable soliton necklaces supported by fractional diffraction and competing nonlinearities, *Opt. Exp.* **28**, 34472-33488 (2020).
- [49] L. Zeng, D. Mihalache, B. A. Malomed, X. Lu, Y. Cai, Q. Zhu, and J. Li, Families of fundamental and multipole solitons in a cubic-quintic nonlinear lattice in fractional dimension, *Chaos Solitons Fract.* **144**, 110589 (2021).
- [50] L. Zeng and J. Zeng, Preventing critical collapse of higher-order solitons by tailoring unconventional optical diffraction and nonlinearities, *Commun. Phys.* **3**, 26 (2020).
- [51] M. I. Molina, The fractional discrete nonlinear Schrödinger equation, *Phys. Lett. A* **384**, 126180 (2020).
- [52] L. Zeng, B. A. Malomed, D. Mihalache, Y. Cai, X. Lu, Q. Zhu, and J. Li, Bubbles and W-shaped solitons in Kerr media with fractional diffraction, *Nonlinear Dynamics* **104**, 4253-4264 (2021).
- [53] J. Thirouin, On the growth of Sobolev norms of solutions of the fractional defocusing NLS equation on the circle, *Ann. Inst. H. Poincaré AN* **34**, 509-531 (2017).
- [54] L. Zeng, Y. Zhu, B. A. Malomed, D. Mihalache, Q. Wang, H. Long, Y. Cai, X. Lu, and J. Li, Quadratic fractional solitons, *Chaos, Solitons & Fractals* **154**, 111586 (2022).
- [55] Y. Qiu, B. A. Malomed, D. Mihalache, X. Zhu, L. Zhang, and Y. He, Soliton dynamics in a fractional complex Ginzburg-Landau model, *Chaos Solitons Fract.* **131**, 109471 (2020).
- [56] M. Romagnoli, S. Trillo, and S. Wabnitz, Soliton switching in nonlinear couplers, *Opt. Quantum Electron* **24**, S1237-S1267 (1992).
- [57] *Spontaneous Symmetry Breaking, Self-Trapping, and Josephson Oscillations*, Editor: B. A. Malomed (Springer-Verlag: Berlin and Heidelberg, 2013).
- [58] E. B. Davies, Symmetry breaking in a non-linear Schrödinger equation, *Commun. Math. Phys.* **64**, 191-210 (1979).
- [59] J. C. Eilbeck, P. S. Lomdahl, and A. C. Scott, The discrete self-trapping equation, *Physica D* **16**, 318-338 (1985).
- [60] G. J. Milburn, J. Corney, E. M. Wright, and D. F. Walls, "Quantum dynamics of an atomic Bose-Einstein condensate in a double-well potential", *Phys. Rev. A* **55**, 4318-4324 (1997).
- [61] A. Smerzi, S. Fantoni, S. Giovanazzi, and S. R. Shenoy, "Quantum coherent atomic tunneling between two trapped Bose-Einstein condensates", *Phys. Rev. Lett.* **79**, 4950-4953 (1997).
- [62] S. Raghavan, A. Smerzi, S. Fantoni, and S. R. Shenoy, Coherent oscillations between two weakly coupled Bose-Einstein condensates: Josephson effects,  $\pi$  oscillations, and macroscopic quantum self-trapping, *Phys. Rev. A* **59**, 620-633 (1999).
- [63] M. Matuszewski, B. A. Malomed, and M. Trippenbach, Spontaneous symmetry breaking of solitons trapped in a double-channel potential, *Phys. Rev. A* **75**, 063621 (2007).
- [64] T. Heil, I. Fischer, W. Elsässer, J. Mulet, and C. R. Mirasso, Chaos synchronization and spontaneous symmetry-breaking in symmetrically delay-coupled semiconductor lasers, *Phys. Rev. Lett.* **86**, 795-798 (2000).
- [65] M. Albiez, R. Gati, J. Fölling, S. Hunsmann, M. Cristiani, and M. K. Oberthaler, Direct observation of tunneling and nonlinear self-trapping in a single bosonic Josephson junction, *Phys. Rev. Lett.* **95**, 010402 (2005).
- [66] P. G. Kevrekidis, Z. Chen, B. A. Malomed, D. J. Frantzeskakis, and M. I. Weinstein, Spontaneous symmetry breaking in photonic lattices: Theory and experiment, *Phys. Lett. A* **340**, 275-280 (2005).

- [67] A. Christ, O. J. F. Martin, Y. Ekinci, N. A. Gippius, and S. G. Tikhodeev, Symmetry breaking in a plasmonic metamaterial at optical wavelength, *Nano Lett.* **8**, 2171-2175 (2008).
- [68] P. Li, and C. Dai, Double loops and pitchfork symmetry breaking bifurcations of optical solitons in nonlinear fractional Schrödinger equation with competing cubic-quintic nonlinearities, *Ann. Phys. (Berlin)* **532**, 2000048 (2020).
- [69] P. Li, B. A. Malomed, and D. Mihalache, Symmetry breaking of spatial Kerr solitons in fractional dimension, *Chaos Solitons Fract.* **132**, 109602 (2020).
- [70] J. Chen and J. Zeng, Spontaneous symmetry breaking in purely nonlinear fractional systems, *Chaos* **30**, 063131 (2020).
- [71] P. Li, R. Li, and C. Dai, Existence, symmetry breaking bifurcation and stability of two-dimensional optical solitons supported by fractional diffraction, *Opt. Exp.* **29**, 3193-3210 (2021).
- [72] B. A. Malomed, Variational methods in nonlinear fiber optics and related fields., *Prog. Optics* **43**, 71-193 (2002).
- [73] B. A. Malomed, A variety of dynamical settings in dual-core nonlinear fibers, In: *Handbook of Optical Fibers*, Vol. 1, pp. 421-474 (G.-D. Peng, Editor: Springer, Singapore, 2019).
- [74] E. M. Wright, G. I. Stegeman, and S. Wabnitz, Solitary-wave decay and symmetry-breaking instabilities in two-mode fibers, *Phys. Rev. A* **40**, 4455-4466 (1989).
- [75] C. Paré and M. Flórjańczyk, Approximate model of soliton dynamics in all-optical couplers, *Phys. Rev. A* **41**, 6287-6295 (1990).
- [76] A. W. Snyder, D. J. Mitchell, L. Poladian, D. R. Rowland, and Y. Chen, Physics of nonlinear fiber couplers, *J. Opt. Soc. Am. B* **8**, 2101-2118 (1991).
- [77] A. I. Maimistov, Propagation of a light pulse in nonlinear tunnel-coupled optical waveguides, *Kvant. Elektron.* **18**, 758-761 [*Sov. J. Quantum Electron.* **21**, 687-690 (1991)].
- [78] N. Akhmediev and A. Ankiewicz, Novel soliton states and bifurcation phenomena in nonlinear fiber couplers, *Phys. Rev. Lett.* **70**, 2395-2398 (1993).
- [79] B. A. Malomed, I. Skinner, P. L. Chu, and G. D. Peng, Symmetric and asymmetric solitons in twin-core nonlinear optical fibers, *Phys. Rev. E* **53**, 4084 (1996).
- [80] V. H. Nguyen, L. X. T. Tai, I. Bugar, M. Longobucco, R. Buzcynski, B. A. Malomed, and M. Trippenbach, Reversible ultrafast soliton switching in dual-core highly nonlinear optical fibers, *Opt. Lett.* **45**, 5221-5224 (2020).
- [81] L. Zeng and J. Zeng, Fractional quantum couplers, *Chaos, Solitons and Fractals* **140**, 110271 (2020).
- [82] G. Iooss and D. D. Joseph, *Elementary Stability Bifurcation Theory* (Springer-Verlag: New York, 1980).
- [83] G. P. Agrawal, *Nonlinear Fiber Optics* (Academic Press, Amsterdam, 2013).
- [84] H. G. Winful and D. T. Walton, Passive-mode locking through nonlinear coupling in a dual-core fiber laser, *Opt. Lett.* **17**, 1688-1690 (1992).
- [85] J. Yang, *Nonlinear Waves in Integrable and Nonintegrable Systems*, SIAM, Philadelphia, 2010.
- [86] J. Yang and T. I. Lakoba, Universally-convergent squared-operator iteration methods for solitary waves in general nonlinear wave equations, *Stud. Appl. Math.* **118**, 153-197 (2007).
- [87] N. G. Vakhitov and A.A. Kolokolov, Stationary solutions of the wave equation in a medium with nonlinearity saturation, *Izv. Vyssh. Uchebn. Zaved., Radiofiz.* **16**, 1020-1028 (1973) [*Radiophys. Quantum Electron.* **16**, 783-789 (1973)].
- [88] T. Maytevarunyoo, B. A. Malomed, and G. Dong, Spontaneous symmetry breaking in a nonlinear double-well structure, *Phys. Rev. A* **78**, 053601 (2008).
- [89] M. Weinstein, Lyapunov stability of ground states of nonlinear dispersive evolution equations, *Comm. Pure Appl. Math.* **39**, 51-67 (1986).
- [90] L. N. Trefethen, *Spectral Method in Matlab*, SIAM, Philadelphia, 2000.
- [91] J. P. Boyd, *Chebyshev and Fourier Spectral Methods*, 2nd ed., Dover, Mineola, NY, 2001.
- [92] B. Guo, X. Pu, and F. Huang, *Fractional Partial Differential Equations and their Numerical Solutions*, World Scientific, Singapore, 2015.
- [93] G. D. Peng, B. A. Malomed, and P. L. Chu, Soliton collisions in a model of a dual-core nonlinear optical fiber, *Phys. Scripta* **58**, 149-158 (1998).
- [94] L. Khaykovich and B. A. Malomed, Deviation from one dimensionality in stationary properties and collisional dynamics of matter-wave solitons, *Phys. Rev. A* **7**, 023607 (2006).
- [95] Yu. S. Kivshar and B. A. Malomed, Dynamics of solitons in nearly integrable systems, *Rev. Mod. Phys.* **61**, 763-915 (1989).
- [96] A. Sigler and B. A. Malomed, Solitary pulses in linearly coupled cubic-quintic Ginzburg-Landau equations, *Physica D* **212**, 305-316 (2005).